

Improved Measurement of CP Violation Parameters in $B_s^0 \rightarrow J/\psi K^+ K^-$ Decays in the Vicinity of the $\phi(1020)$ Resonance

R. Aaij *et al.*^{*}
(LHCb Collaboration)



(Received 4 August 2023; accepted 4 December 2023; published 2 February 2024; corrected 14 February 2024)

The decay-time-dependent CP asymmetry in $B_s^0 \rightarrow J/\psi(\rightarrow \mu^+\mu^-)K^+K^-$ decays is measured using proton-proton collision data, corresponding to an integrated luminosity of 6 fb^{-1} , collected with the LHCb detector at a center-of-mass energy of 13 TeV . Using a sample of approximately $349\,000 B_s^0$ signal decays with an invariant K^+K^- mass in the vicinity of the $\phi(1020)$ resonance, the CP -violating phase ϕ_s is measured, along with the difference in decay widths of the light and heavy mass eigenstates of the B_s^0 - \bar{B}_s^0 system, $\Delta\Gamma_s$, and the difference of the average B_s^0 and B^0 meson decay widths, $\Gamma_s - \Gamma_d$. The values obtained are $\phi_s = -0.039 \pm 0.022 \pm 0.006 \text{ rad}$, $\Delta\Gamma_s = 0.0845 \pm 0.0044 \pm 0.0024 \text{ ps}^{-1}$, and $\Gamma_s - \Gamma_d = -0.0056^{+0.0013}_{-0.0015} \pm 0.0014 \text{ ps}^{-1}$, where the first uncertainty is statistical and the second systematic. These are the most precise single measurements to date and are consistent with expectations based on the Standard Model and with the previous LHCb analyses of this decay. These results are combined with previous independent LHCb measurements. The phase ϕ_s is also measured independently for each polarization state of the K^+K^- system and shows no evidence for polarization dependence.

DOI: 10.1103/PhysRevLett.132.051802

The interference between B_s^0 -mixing and -decay amplitudes to CP eigenstates with a $c\bar{c}$ resonance in the final state gives rise to a measurable CP -violating phase ϕ_s , which is particularly sensitive to physics beyond the standard model (SM). In the SM, neglecting subleading loop contributions in $b \rightarrow c\bar{c}s$ transitions, ϕ_s is predicted to be equal to $-2\beta_s$, where $\beta_s \equiv \arg [-(V_{ts}V_{tb}^*)/(V_{cs}V_{cb}^*)]$ and V_{ij} are elements of the Cabibbo-Kobayashi-Maskawa (CKM) quark-flavor-mixing matrix [1]. Global fits to experimental data, under the assumption of the CKM paradigm, give $-2\beta_s = -0.0368^{+0.0009}_{-0.0006} \text{ rad}$ [2]. This precise indirect determination makes the measurement of ϕ_s an excellent probe for physics beyond the SM, especially for models contributing to B_s^0 - \bar{B}_s^0 mixing [3,4]. Several experiments have measured ϕ_s , the B_s^0 decay width, and decay-width difference, Γ_s and $\Delta\Gamma_s$, respectively, in B_s^0 decays via $b \rightarrow c\bar{c}s$ transitions [5–19]. The measurements lead to the current world average of $\phi_s^{c\bar{c}s} = -0.049 \pm 0.019 \text{ rad}$ [20], which is dominated by the LHCb results in $B_s^0 \rightarrow J/\psi h^+h^-$ ($h = K, \pi$) decays using 5 fb^{-1} of data collected at center-of-mass energies of $\sqrt{s} = 7, 8$, and 13 TeV [13]. This Letter reports an update of the LHCb

measurements in $B_s^0 \rightarrow J/\psi K^+K^-$ decays [21] using the full Run 2 data taken in 2015–2018, corresponding to an integrated luminosity of 6 fb^{-1} at $\sqrt{s} = 13 \text{ TeV}$. The results supersede those in Ref. [13] and are combined with the LHCb result using 3 fb^{-1} of Run 1 data [12]. Apart from the increased data size, this analysis benefits from improvements in the calibration procedures of the particle identification (PID), flavor-tagging algorithms, and the B_s^0 decay-time resolution model.

The LHCb detector is a single-arm forward spectrometer covering the pseudorapidity range $2 < \eta < 5$, described in detail in Refs. [22,23]. Simulated events produced with the software described in Refs. [24–27] are used to model the effects of the detector acceptance, resolution, and selection requirements. Dedicated simulations are produced for each year of data taking corresponding to the relevant detector and accelerator conditions. High-purity data samples of charm hadron, charmonia, and beauty hadron decays are used to calibrate the simulated single-particle reconstruction and PID efficiencies. The trigger, which performs the online data selection [28], consists of a hardware stage, based on the high transverse momentum, p_T , and signatures from the calorimeter and muon systems, followed by a software stage with full event reconstruction. Two software trigger algorithms, exploiting the muon kinematics and two-muon vertex information, are used to select candidates. The first requires a vertex with a large impact-parameter significance from all primary vertexes and, therefore, introduces a nontrivial efficiency dependence on the B_s^0 decay time. The second has almost uniform decay-time efficiency.

*Full author list given at the end of the Letter.

Published by the American Physical Society under the terms of the Creative Commons Attribution 4.0 International license. Further distribution of this work must maintain attribution to the author(s) and the published article's title, journal citation, and DOI. Funded by SCOAP³.

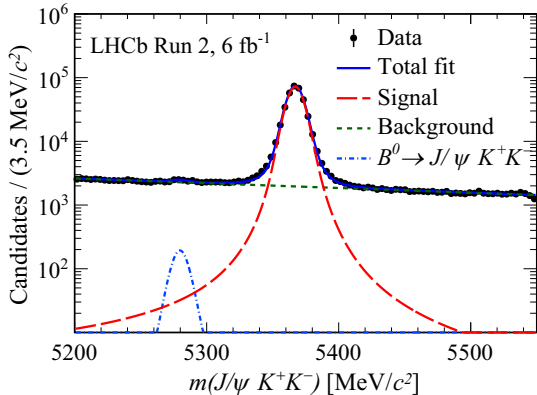


FIG. 1. Distribution of $m(J/\psi K^+ K^-)$ for the full data sample and projection of the maximum likelihood fit.

Consequently, candidates selected by the two triggers are studied in separate categories.

The selection of $B_s^0 \rightarrow J/\psi(\rightarrow \mu^+\mu^-)K^+K^-$ candidates, with K^+K^- invariant masses in the range [990, 1050] MeV/c^2 , follows the same strategy used in the previous Run 2 measurement [13]. In order to take into account different data-taking and calibration conditions for optimal event selection, a gradient-boosted decision tree (BDT) classifier applied in the selection is trained separately for each year between 2016 and 2018, with the result for 2016 applied to the 2015 dataset due to its limited size. The BDT selection improves the signal-to-background ratio by about a factor of 50. The peaking backgrounds due to pion and proton misidentification in B^0 and Λ_b^0 decays are significantly reduced with stringent PID and mass requirements. The remaining peaking background from $\Lambda_b^0 \rightarrow J/\psi p K^-$ decays is subtracted statistically through the injection of simulated events into the data with a negative sum of weights equal to the expected number of 4700 Λ_b^0 candidates.

Selected $B_s^0 \rightarrow J/\psi K^+K^-$ candidates in the mass range [5200, 5550] MeV/c^2 are subsequently retained for analysis. The data sample is divided into 48 independent subsamples, corresponding to six $m(K^+K^-)$ bins with boundaries at 990, 1008, 1016, 1020, 1024, 1032, and 1050 MeV/c^2 , two trigger categories, and four years of data taking. The invariant mass of selected B_s^0 candidates, $m(J/\psi K^+ K^-)$, and the per-candidate mass uncertainty σ_m are calculated by constraining the J/ψ mass to the world average [20] and requiring the B_s^0 candidate momentum to point back to the corresponding primary vertex. Using $m(J/\psi K^+ K^-)$ as the discriminating variable, a signal weight is assigned to each candidate with the sPlot method [29–31], using an extended maximum-likelihood fit, shown in Fig. 1. The signal shape is described by a double-sided Crystal Ball (CB) function [32], whose width is parametrized as a function of σ_m , using a second-order polynomial. This parametrization accounts for the correlation between

$m(J/\psi K^+ K^-)$ and the helicity angle $\cos \theta_\mu$, which is due to the dependence of the $m(J/\psi K^+ K^-)$ resolution, characterized by σ_m , on the p_T of the muons. Since the muon p_T depends on $\cos \theta_\mu$, σ_m is found to represent a good proxy for $\cos \theta_\mu$. The parameters that describe the tail of the CB function are fixed to those obtained from simulation. The background from $B^0 \rightarrow J/\psi K^+ K^-$ decays is modeled with the same CB function as the signal, sharing all shape parameters except for the mean of the distribution. The difference between the means of the signal and B^0 components is fixed to its world average [20]. The background due to random combinations of tracks is modeled with an exponential function. The peaking background from $B^0 \rightarrow J/\psi K^+ \pi^-$ decays is estimated to be negligible. The $B_s^0 \rightarrow J/\psi K^+ K^-$ signal yields are 16181 ± 135 , 103319 ± 342 , 105465 ± 343 , and 123870 ± 476 for the 2015, 2016, 2017, and 2018 datasets, respectively.

The measurement of ϕ_s in $B_s^0 \rightarrow J/\psi K^+ K^-$ decays requires the CP -even and CP -odd decay-amplitude components to be disentangled, depending upon the relative orbital angular momentum between the J/ψ candidate and the kaon pair. A weighted simultaneous fit to the distributions of decay time and decay angles ($\cos \theta_K$, $\cos \theta_\mu$, ϕ_h) in the helicity basis, as described in Ref. [13], is performed for the 48 independent subsamples, to determine the physics parameters. These parameters are ϕ_s ; $|\lambda|$; $\Gamma_s - \Gamma_d$; $\Delta\Gamma_s$; the B_s^0 mass difference Δm_s ; and the polarization amplitudes $A_k = |A_k|e^{-i\delta_k}$, where the indices $k \in \{0, \parallel, \perp, S\}$ refer to the different polarization states of the K^+K^- system. The sum $|A_\parallel|^2 + |A_0|^2 + |A_\perp|^2$ equals unity, and δ_0 is zero, by convention. The parameter λ is defined as $\eta_k(q/p)(\bar{A}_k/A_k)$, where $p = \langle B_s^0 | B_L \rangle$ and $q = \langle \bar{B}_s^0 | B_L \rangle$ describe the relation between mass and flavor eigenstates and η_k is the CP eigenvalue of the polarization state k .

The probability density function (PDF) for the signal in each subsample accounts for the decay-time resolution, the decay-time and angular efficiencies, and the flavor tagging. It considers P - and S -wave components of the kaon pair from $\phi(1020)$ and $f_0(980)$ decays, while the D -wave component is neglected [15,33]. The interference of P and S waves includes an effective coupling factor C_{SP} , determined in each $m(K^+K^-)$ bin through integration of the mass line shape interference term. The line shape of the $\phi(1020)$ resonance [15,33] is modeled as a relativistic Breit-Wigner distribution, while the $f_0(980)$ resonance is modeled as a Flatté amplitude with parameters from Ref. [34]. The effect of mass resolution is also accounted for. The computed values of C_{SP} are 0.8458 ± 0.0018 , 0.8673 ± 0.0004 , 0.8127 ± 0.0012 , 0.8558 ± 0.0010 , 0.9359 ± 0.0004 , and 0.9735 ± 0.0001 from the lowest to the highest $m(K^+K^-)$ bin. The value of Γ_d is fixed to its world average [35]. All physics parameters are left unconstrained in the fit and are shared across the subsamples, except for the S -wave fraction and the phase difference

$\delta_s - \delta_\perp$, which are independent parameters for each $m(K^+K^-)$ bin.

The experimental decay-time resolution is accounted for by convolving the signal PDF with a Gaussian resolution function with the per-candidate decay-time uncertainty as the width. The per-candidate decay-time uncertainty is calibrated to represent the effective resolution, which is determined from a control sample of promptly decaying J/ψ candidates combined with two kaons selected similarly as the signal except for the decay time and flight distance requirements. The candidates with negative reconstructed decay times, arising from purely detector resolution effects, are used for the calibration. The possible contamination from nonprompt decays is estimated to be around 1%–2% and has a negligible effect on the calibration model. The average resolution for the signal candidates is determined to be around 42 fs.

The prompt sample used in the decay-time resolution calibration has a nonzero mean decay time due to residual detector misalignment. This bias, which depends on the kinematics, is corrected for in the analysis. In the misaligned simulated samples, a small bias remains after the correction and is assigned as a systematic uncertainty.

The reconstruction and selection produce a nonuniform efficiency as a function of the decay time and angles of the B_s^0 decays. The angular and decay-time efficiencies are assumed to factorize and are evaluated separately for different years of data taking and for the two trigger categories. The three-dimensional angular efficiency correction is introduced through normalization weights in the PDF describing the signal decays in the time-dependent angular fit. The efficiency is determined from simulated signal events subjected to the same selection criteria as data. The simulated sample is corrected by an iterative procedure using data [13].

The decay-time efficiency is determined using a data-driven method with a reference channel $B^0 \rightarrow J/\psi K^{*0} (\rightarrow K^+ \pi^-)$ that is topologically similar to the signal channel. The decay-time efficiency is modeled by a cubic spline function, determined from the decay-time distribution of selected candidates divided by the expected distribution for the case of perfect acceptance. The latter is modeled by an exponential distribution with the B^0 lifetime [20], convolved with a Gaussian resolution function with a width of 42 fs. Simulated B^0 and B_s^0 events are used to determine and apply corrections at the level of 3% to account for kinematic differences between B^0 and B_s^0 decays. The background-subtracted $B^0 \rightarrow J/\psi K^{*0}$ candidates are selected using the same strategy as in Ref. [13], with an additional requirement on the helicity angle $\cos \theta_K < 0$, to avoid a large difference between signal and control samples, since pions with $\cos \theta_K > 0$ tend to have extremely low momenta. The decay-time efficiency is validated by replacing B_s^0 samples with B^+ and B^0 samples

TABLE I. Main physics parameters of interest, where the first uncertainty is statistical and the second systematic.

Parameter	Values
ϕ_s [rad]	$-0.039 \pm 0.022 \pm 0.006$
$ \lambda $	$1.001 \pm 0.011 \pm 0.005$
$\Gamma_s - \Gamma_d [\text{ps}^{-1}]$	$-0.0056^{+0.0013}_{-0.0015} \pm 0.0044 \pm 0.0014$
$\Delta\Gamma_s [\text{ps}^{-1}]$	$0.0845 \pm 0.0044 \pm 0.0024$
$\Delta m_s [\text{ps}^{-1}]$	$17.743 \pm 0.033 \pm 0.009$
$ A_\perp ^2$	$0.2463 \pm 0.0023 \pm 0.0024$
$ A_0 ^2$	$0.5179 \pm 0.0017 \pm 0.0032$
$\delta_\perp - \delta_0$ [rad]	$2.903^{+0.075}_{-0.074} \pm 0.048$
$\delta_\parallel - \delta_0$ [rad]	$3.146 \pm 0.061 \pm 0.052$

where the decay widths are measured to be consistent with their corresponding world averages [20].

The flavor of the B_s^0 meson at production is inferred using two independent classes of flavor-tagging algorithms, the opposite-side (OS) tagger [36] and same-side (SS) tagger [37], which exploit specific accompanying B meson decays and signal fragmentation information, respectively. Each method yields a tagging decision Q , with an estimated mistag probability κ , for each B_s^0 meson, where $Q = +1, -1$, or 0, if the meson is classified as B_s^0, \bar{B}_s^0 , or untagged, respectively. To obtain the correct mistag probability ω , each algorithm is calibrated using a linear function following the same strategy as Ref. [13]. The calibration of the OS mistag probability uses $B^+ \rightarrow J/\psi K^+$ decays, for which the value of ω in an interval of κ can be obtained from the number of correct and wrong decisions. The calibration of the SS mistag probability uses flavor-specific $B_s^0 \rightarrow D_s^- \pi^+$ decays, for which the value of ω in an interval of κ is estimated by fitting the decay-time distribution. The decay-time acceptance is modeled with a cubic spline [38]. The effective tagging power is given by the product of the tagging efficiency (ϵ_{tag}) and the wrong-tag dilution squared, $\epsilon_{\text{tag}} \times (1 - 2\omega)^2$. The combined tagging powers of the OS and SS taggers are $(4.18 \pm 0.15)\%$, $(4.22 \pm 0.16)\%$, and $(4.36 \pm 0.16)\%$ for 2015–2016, 2017, and 2018, respectively, where the statistical and systematic uncertainties are combined. A novel inclusive flavor-tagging algorithm [39], which uses track information from the full event, is applied as an alternative method to cross-check the OS and SS combined method and provides compatible results for ϕ_s with similar precision.

The results of the simultaneous maximum likelihood fit to the 48 independent data samples for the nine main physics parameters of interest are given in Table I. The statistical uncertainties are computed using the profile-likelihood method and cross-checked with the bootstrapping technique [40,41]. The background-subtracted data distributions with fit projections are shown in Fig. 2. The results are in good agreement with the LHCb Run 1 and 2015–2016 measurements [12–14]. As a cross-check, the

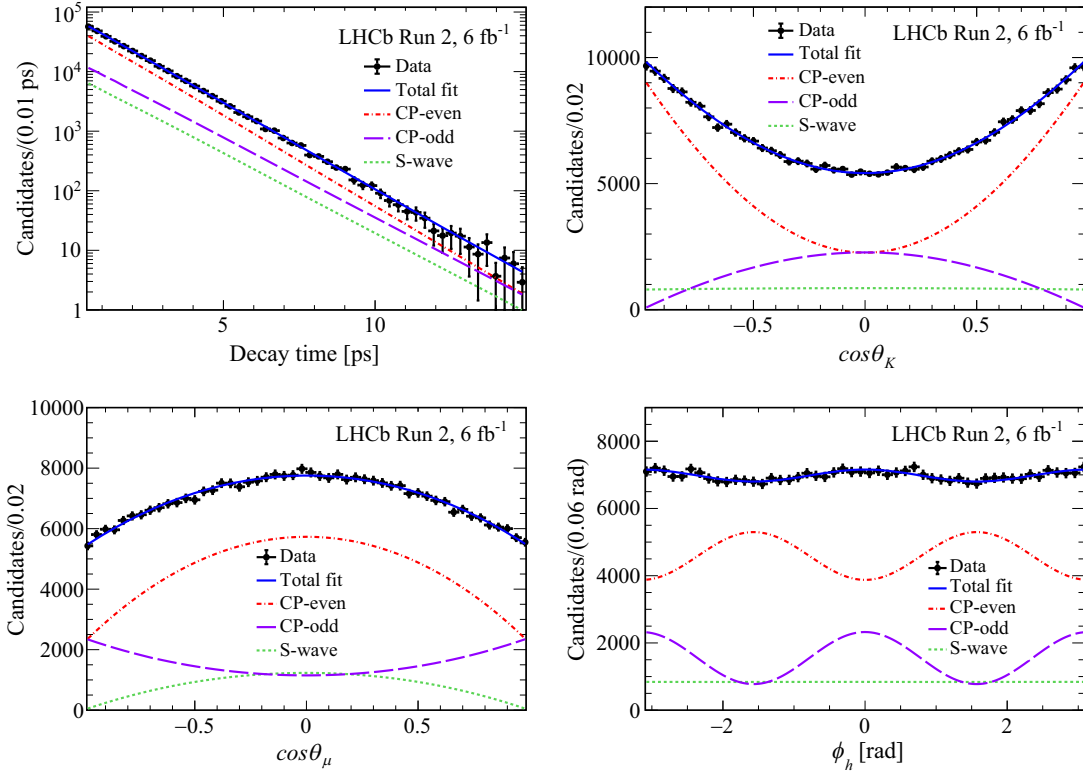


FIG. 2. Decay-time and decay-angle distributions for background-subtracted $B_s^0 \rightarrow J/\psi K^+ K^-$ decays with the one-dimensional projections of the PDF at the maximum-likelihood point. The data and fit projections for the different samples considered [data-taking year, trigger and tagging categories, $m(K^+ K^-)$ bins] are combined.

analysis is performed on the 2015–2016 data subsample, and the results are consistent with the previous Run 2 measurement [13]. The measurements of ϕ_s , $\Delta\Gamma_s$, and $\Gamma_s - \Gamma_d$ are the most precise to date and agree with the SM expectations [2,42–44]. No CP violation in $B_s^0 \rightarrow J/\psi K^+ K^-$ decays is found. The value of Δm_s agrees with the world average [20]. The amplitudes of the S -wave component are determined in the same fit and summarized in Supplemental Material [45]. Removing the assumption that the CP -violating parameters $|\lambda|$ and ϕ_s are the same for all polarization states shows no evidence for any polarization dependence, and the corresponding results are summarized in Table II.

The total systematic uncertainties shown in Table I are the quadrature sum of different contributions, described in the following and summarized in Supplemental Material [45]. The tagging parameters are constrained in the fit, and, therefore, their associated systematic uncertainties contribute to the statistical uncertainty of each physics parameter. This contribution is 0.0025 rad to ϕ_s and 0.0015 ps⁻¹ to Δm_s and is negligible for all other parameters.

The systematic uncertainties related to the mass fit model are estimated by changing the calibration model of the per-candidate mass uncertainty, varying the estimation of misidentified Λ_b^0 and mass resolution parameters independently. The signal weights are recomputed by varying the fit

parameters within their statistical uncertainties. Since the sPlot method implicitly relies on factorization of the discriminating variable, $m(J/\psi K^+ K^-)$, and the rest of the observables, a systematic uncertainty is assigned for the small correlation between the $m(J/\psi K^+ K^-)$ distribution and the decay time and angles by reevaluating the signal weights in bins of decay time and angles. The effect of ignoring the contribution of $B_c^+ \rightarrow B_s^0 X$ candidates is evaluated with pseudoexperiments by adding about 2% [46–48] of $B_c^+ \rightarrow B_s^0 (\rightarrow J/\psi \phi) X$ simulated candidates, estimated from the branching fraction and efficiencies.

TABLE II. Measured observables in the polarization-dependent fit. The uncertainties are statistical only.

Parameters	Values
ϕ_s^0 [rad]	-0.034 ± 0.023
$\phi_s^\parallel - \phi_s^0$ [rad]	-0.002 ± 0.021
$\phi_s^\perp - \phi_s^0$ [rad]	$-0.001^{+0.020}_{-0.021}$
$\phi_s^S - \phi_s^0$ [rad]	$0.022^{+0.027}_{-0.026}$
$ \lambda^0 $	$0.969^{+0.025}_{-0.024}$
$ \lambda^\parallel/\lambda^0 $	$0.982^{+0.055}_{-0.052}$
$ \lambda^\perp/\lambda^0 $	$1.107^{+0.082}_{-0.076}$
$ \lambda^S/\lambda^0 $	$1.121^{+0.084}_{-0.078}$

The B_c^+ component causes biases in Γ_s and $\Delta\Gamma_s$ at the level of about 0.0015 ps^{-1} . These are corrected for in the final fit taking into account the systematic uncertainty on the bias, while minor differences in other parameters are taken as systematic uncertainties. The effect of neglecting a possible D -wave K^+K^- component is conservatively estimated with pseudoexperiments that contain twice the size of the expected D -wave contribution from Ref. [33].

The effect due to imperfect removal of ghost tracks [49] reconstructed with noisy hits is evaluated according to simulation and considered among the systematic uncertainties. Around 1.4% of the selected events have multiple candidates; the effect of such cases is considered in systematic uncertainties by choosing one candidate randomly and repeating the fit. Systematic uncertainties are assigned due to the limited size of the PID calibration samples. Different models of the S -wave line shape based on the results in Ref. [34] are used to evaluate the C_{SP} factors and assign systematic uncertainties.

A systematic uncertainty for the translation of the decay-time resolution calibration from the control sample to signal is derived using simulation. A minor systematic uncertainty due to non-Gaussian effects in the decay-time resolution is assigned. Systematic uncertainties accounting for the limited sizes of the calibration sample for the decay-time resolution and the simulated samples for the angular efficiencies are estimated by varying the calibration parameters and efficiencies according to the statistical covariance matrices. The effect of ignoring the angular resolutions in the fit is estimated by performing separate fits to the generated and reconstructed angular variables from simulation, and the differences are taken as systematic uncertainties. The effect of the specific configuration of the gradient-boosted tree method applied to correct the kinematics of simulation in the time and angular efficiency is estimated by applying 100 alternative configurations.

The longitudinal scale of the vertex detector has a relative uncertainty of 0.022% [50,51], and a systematic uncertainty is assigned by scaling the track parameters with this uncertainty. The systematic uncertainty associated with the track momentum scale calibration is estimated by varying all track momenta by 0.03% [52]. Possible biases in the fitting procedure and effects of neglecting correlations between the decay-angle and decay-time efficiencies are studied using pseudoexperiments. The results are found to be stable when repeating the analysis on subsets of the data, split by the two LHCb magnet polarities, trigger conditions, year of data taking, number of reconstructed primary vertices, bins of $B_s^0 p_T$, η , or tagging categories.

In conclusion, the CP -violation and decay-width parameters in the decay $B_s^0 \rightarrow J/\psi K^+K^-$ are measured using the full Run 2 dataset collected by the LHCb experiment. The results are $\phi_s = -0.039 \pm 0.022 \pm 0.006 \text{ rad}$, $|\lambda| = 1.001 \pm 0.011 \pm 0.005$, $\Gamma_s - \Gamma_d = -0.0056^{+0.0013}_{-0.0015} \pm 0.0014 \text{ ps}^{-1}$, and $\Delta\Gamma_s = 0.0845 \pm 0.0044 \pm 0.0024 \text{ ps}^{-1}$, superseding

the previous Run 2 LHCb measurement in the same decay [13]. No evidence for CP violation is found in the $B_s^0 \rightarrow J/\psi(\mu^+\mu^-)K^+K^-$ decay. The results are consistent with the previous measurements in $B_s^0 \rightarrow J/\psi(\mu^+\mu^-)K^+K^-$ [12,13] and $B_s^0 \rightarrow J/\psi(e^+e^-)K^+K^-$ [14] decays and the combination with which yields $\phi_s = -0.044 \pm 0.020 \text{ rad}$ and $|\lambda| = 0.990 \pm 0.010$. A combination of all LHCb ϕ_s measurements in B_s^0 decays via $b \rightarrow c\bar{c}s$ transitions [12,14–16,18,19], $B_s^0 \rightarrow J/\psi(\mu^+\mu^-)K^+K^-$ above the $\phi(1020)$ resonance, $B_s^0 \rightarrow D_s^+D_s^+$, $B_s^0 \rightarrow J/\psi\pi^+\pi^-$, $B_s^0 \rightarrow \psi(2S)K^+K^-$, and $B_s^0 \rightarrow J/\psi K^+K^-$, yields $\phi_s = -0.031 \pm 0.018 \text{ rad}$. The full fit results and correlations are provided in Supplemental Material [45]. This is the most precise measurement of the CP -violating phase ϕ_s to date and is consistent with SM predictions [2,42].

We express our gratitude to our colleagues in the CERN accelerator departments for the excellent performance of the LHC. We thank the technical and administrative staff at the LHCb institutes. We acknowledge support from CERN and from the national agencies: CAPES, CNPq, FAPERJ, and FINEP (Brazil); MOST and NSFC (China); CNRS/IN2P3 (France); BMBF, DFG, and MPG (Germany); INFN (Italy); NWO (Netherlands); MNiSW and NCN (Poland); MCID/IFA (Romania); MICINN (Spain); SNSF and SER (Switzerland); NASU (Ukraine); STFC (United Kingdom); DOE NP and NSF (USA). We acknowledge the computing resources that are provided by CERN, IN2P3 (France), KIT and DESY (Germany), INFN (Italy), SURF (Netherlands), PIC (Spain), GridPP (United Kingdom), CSCS (Switzerland), IFIN-HH (Romania), CBPF (Brazil), Polish WLCG (Poland), and NERSC (USA). We are indebted to the communities behind the multiple open-source software packages on which we depend. Individual groups or members have received support from ARC and ARDC (Australia); Minciencias (Colombia); AvH Foundation (Germany); EPLANET, Marie Skłodowska-Curie Actions, ERC, and NextGenerationEU (European Union); A*MIDEX, ANR, IPhU and Labex P2IO, and Région Auvergne-Rhône-Alpes (France); Key Research Program of Frontier Sciences of CAS, CAS PIFI, CAS CCEPP, Fundamental Research Funds for the Central Universities, and Sci. & Tech. Program of Guangzhou (China); GVA, XuntaGal, GENCAT, Inditex, InTalent and Prog. Atracción Talento, CM (Spain); SRC (Sweden); the Leverhulme Trust, the Royal Society and UKRI (United Kingdom).

[1] M. Kobayashi and T. Maskawa, CP -violation in the renormalizable theory of weak interaction, *Prog. Theor. Phys.* **49**, 652 (1973); N. Cabibbo, Unitary symmetry and leptonic decays, *Phys. Rev. Lett.* **10**, 531 (1963).

- [2] J. Charles *et al.* (CKMfitter group), Current status of the standard model CKM fit and constraints on $\Delta F = 2$ new physics, *Phys. Rev. D* **91**, 073007 (2015), updated results and plots available at <http://ckmfitter.in2p3.fr/>.
- [3] A. J. Buras, Flavour theory: 2009, *Proc. Sci. EPS-HEP2009* (**2009**) 024 [[arXiv:0910.1032](https://arxiv.org/abs/0910.1032)].
- [4] B. Dutta and Y. Mimura, Large phase of B_s^0 - \bar{B}_s^0 mixing in supersymmetric grand unified theories, *Phys. Rev. D* **78**, 071702(R) (2008).
- [5] T. Aaltonen *et al.* (CDF Collaboration), Measurement of the bottom-strange meson mixing phase in the full CDF data set, *Phys. Rev. Lett.* **109**, 171802 (2012).
- [6] V. M. Abazov *et al.* (D0 Collaboration), Measurement of the CP -violating phase $\phi_s^{J/\psi\phi}$ using the flavor-tagged decay $B_s^0 \rightarrow J/\psi\phi$ in 8 fb^{-1} of $p\bar{p}$ collisions, *Phys. Rev. D* **85**, 032006 (2012).
- [7] G. Aad *et al.* (ATLAS Collaboration), Flavour tagged time dependent angular analysis of the $B_s \rightarrow J/\psi\phi$ decay and extraction of $\Delta\Gamma_s$ and the weak phase ϕ_s in ATLAS, *Phys. Rev. D* **90**, 052007 (2014).
- [8] G. Aad *et al.* (ATLAS Collaboration), Measurement of the CP -violating phase ϕ_s and the B_s^0 meson decay width difference with $B_s^0 \rightarrow J/\psi\phi$ decays in ATLAS, *J. High Energy Phys.* **08** (2016) 147.
- [9] G. Aad *et al.* (ATLAS Collaboration), Measurement of the CP -violating phase ϕ_s in $B_s^0 \rightarrow J/\psi\phi$ decays in ATLAS at 13 TeV, *Eur. Phys. J. C* **81**, 342 (2021).
- [10] V. Khachatryan *et al.* (CMS Collaboration), Measurement of the CP -violating weak phase ϕ_s and the decay width difference $\Delta\Gamma_s$ using the $B_s^0 \rightarrow J/\psi\phi(1020)$ decay channel in pp collisions at $\sqrt{s} = 8$ TeV, *Phys. Lett. B* **757**, 97 (2016).
- [11] A. M. Sirunyan *et al.* (CMS Collaboration), Measurement of the CP -violating phase ϕ_s in the $B_s^0 \rightarrow J/\psi\phi(1020) \rightarrow \mu^+\mu^- K^+ K^-$ channel in proton-proton collisions at $\sqrt{s} = 13$ TeV, *Phys. Lett. B* **816**, 136188 (2021).
- [12] R. Aaij *et al.* (LHCb Collaboration), Precision measurement of CP violation in $B_s^0 J/\psi K^+ K^-$ decays, *Phys. Rev. Lett.* **114**, 041801 (2015).
- [13] R. Aaij *et al.* (LHCb Collaboration), Updated measurement of time-dependent CP -violating observables in $B_s^0 \rightarrow J/\psi K^+ K^-$ decays, *Eur. Phys. J. C* **79**, 706 (2019); **80**, 601(E) (2020).
- [14] R. Aaij *et al.* (LHCb Collaboration), First measurement of the CP -violating phase in $B_s^0 \rightarrow J/\psi(e^+e^-)\phi$ decays, *Eur. Phys. J. C* **81**, 1026 (2021).
- [15] R. Aaij *et al.* (LHCb Collaboration), Resonances and CP -violation in B_s^0 and $\bar{B}_s^0 \rightarrow J/\psi K^+ K^-$ decays in the mass region above the $\phi(1020)$, *J. High Energy Phys.* **08** (2017) 037.
- [16] R. Aaij *et al.* (LHCb Collaboration), Measurement of the CP -violating phase ϕ_s in $\bar{B}_s^0 \rightarrow J/\psi\pi^+\pi^-$ decays, *Phys. Lett. B* **736**, 186 (2014).
- [17] R. Aaij *et al.* (LHCb Collaboration), Measurement of the CP -violating phase ϕ_s from $B_s^0 \rightarrow J/\psi\pi^+\pi^-$ decays in 13 TeV pp collisions, *Phys. Lett. B* **797**, 134789 (2019).
- [18] R. Aaij *et al.* (LHCb Collaboration), Measurement of the CP violating phase and decay-width difference in $B_s^0 \rightarrow \psi(2S)\phi$ decays, *Phys. Lett. B* **762**, 253 (2016).
- [19] R. Aaij *et al.* (LHCb Collaboration), Measurement of the CP -violating phase ϕ_s in $B_s^0 \rightarrow D_s^+ D_s^-$ decays, *Phys. Rev. Lett.* **113**, 211801 (2014).
- [20] R. L. Workman *et al.* (Particle Data Group), Review of particle physics, *Prog. Theor. Exp. Phys.* **2022**, 083C01 (2022).
- [21] The inclusion of charge-conjugate processes is implied throughout this Letter, unless otherwise noted.
- [22] A. A. Alves Jr. *et al.* (LHCb Collaboration), The LHCb detector at the LHC, *J. Instrum.* **3**, S08005 (2008).
- [23] R. Aaij *et al.* (LHCb Collaboration), LHCb detector performance, *Int. J. Mod. Phys. A* **30**, 1530022 (2015).
- [24] T. Sjöstrand, S. Mrenna, and P. Skands, A brief introduction to PYTHIA 8.1, *Comput. Phys. Commun.* **178**, 852 (2008); T. Sjöstrand, S. Mrenna, and P. Skands, PYTHIA 6.4 physics and manual, *J. High Energy Phys.* **05** (2006) 026.
- [25] I. Belyaev *et al.*, Handling of the generation of primary events in Gauss, the LHCb simulation framework, *J. Phys. Conf. Ser.* **331**, 032047 (2011).
- [26] D. J. Lange, The EvtGen particle decay simulation package, *Nucl. Instrum. Methods Phys. Res., Sect. A* **462**, 152 (2001).
- [27] N. Davidson, T. Przedzinski, and Z. Was, PHOTOS interface in c++: Technical and physics documentation, *Comput. Phys. Commun.* **199**, 86 (2016).
- [28] R. Aaij *et al.*, The LHCb trigger and its performance in 2011, *J. Instrum.* **8**, P04022 (2013).
- [29] M. Pivk and F. R. L. Diberder, sPlot: A statistical tool to unfold data distributions, *Nucl. Instrum. Methods Phys. Res., Sect. A* **555**, 356 (2005).
- [30] Y. Xie, sFit: A method for background subtraction in maximum likelihood fit, [arXiv:0905.0724](https://arxiv.org/abs/0905.0724).
- [31] H. Dembinski, M. Kenzie, C. Langenbruch, and M. Schmelling, Custom orthogonal weight functions (COWs) for event classification, *Nucl. Instrum. Methods Phys. Res., Sect. A* **1040**, 167270 (2022).
- [32] T. Skwarnicki, A study of the radiative cascade transitions between the Upsilon-prime and Upsilon resonances, Ph.D. thesis, Institute of Nuclear Physics, Krakow, 1986, <http://inspirehep.net/record/230779>.
- [33] R. Aaij *et al.* (LHCb Collaboration), Amplitude analysis and branching fraction measurement of $\bar{B}_s^0 \rightarrow J/\psi K^+ K^-$, *Phys. Rev. D* **87**, 072004 (2013).
- [34] R. Aaij *et al.* (LHCb Collaboration), Measurement of resonant and CP components in $\bar{B}_s^0 \rightarrow J/\psi\pi^+\pi^-$ decays, *Phys. Rev. D* **89**, 092006 (2014).
- [35] Y. Amhis *et al.* (Heavy Flavor Averaging Group), Averages of b -hadron, c -hadron, and τ -lepton properties as of 2021, *Phys. Rev. D* **107**, 052008 (2023).
- [36] R. Aaij *et al.* (LHCb Collaboration), Opposite-side flavour tagging of B mesons at the LHCb experiment, *Eur. Phys. J. C* **72**, 2022 (2012).
- [37] R. Aaij *et al.* (LHCb Collaboration), A new algorithm for identifying the flavour of B_s^0 mesons at LHCb, *J. Instrum.* **11**, P05010 (2016).
- [38] R. Aaij *et al.* (LHCb Collaboration), Precise determination of the B_s^0 - \bar{B}_s^0 oscillation frequency, *Nat. Phys.* **18**, 1 (2022).
- [39] T. Likhomanenko, D. Derkach, and A. Rogozhnikov, Inclusive flavour tagging algorithm, *J. Phys. Conf. Ser.* **762**, 012045 (2016).

- [40] B. Efron, Bootstrap methods: Another look at the Jackknife, *Ann. Stat.* **7**, 1 (1979).
- [41] C. Langenbruch, Parameter uncertainties in weighted unbinned maximum likelihood fits, *Eur. Phys. J. C* **82**, 393 (2022).
- [42] A. Lenz and G. Teltlalmatzi-Xolocotzi, Model-independent bounds on new physics effects in non-leptonic tree-level decays of B-mesons, *J. High Energy Phys.* **07** (2020) 177.
- [43] M. Artuso, G. Borissov, and A. Lenz, CP violation in the B_s^0 system, *Rev. Mod. Phys.* **88**, 045002 (2016).
- [44] M. Kirk, A. Lenz, and T. Rauh, Dimension-six matrix elements for meson mixing and lifetimes from sum rules, *J. High Energy Phys.* **12** (2017) 068.
- [45] See Supplemental Material at <http://link.aps.org/supplemental/10.1103/PhysRevLett.132.051802> for a summary of systematic uncertainties and numerical results and additional plots for the fit result and combinations of LHCb measurements.
- [46] R. Aaij *et al.* (LHCb Collaboration), Measurement of the B_c^- production fraction and asymmetry in 7 and 13 TeV $p\bar{p}$ collisions, *Phys. Rev. D* **100**, 112006 (2019).
- [47] R. Aaij *et al.* (LHCb Collaboration), Precise measurement of the f_s/f_d ratio of fragmentation fractions and of B_s^0 decay branching fractions, *Phys. Rev. D* **104**, 032005 (2021).
- [48] V. V. Kiselev, Decays of the B_c meson, arXiv:hep-ph/0308214.
- [49] P. Li, E. Rodrigues, and S. Stahl, Tracking definitions and conventions for Run 3 and beyond, Reports No. LHCb-PUB-2021-005, No. CERN-LHCb-PUB-2021-005, 2021, <http://cdsweb.cern.ch/search?p=LHCb-PUB-2021-005>; CERN-LHCb-PUB-2021-005&f=reportnumber&action_search=Search&c=LHCb+Notes.
- [50] R. Aaij *et al.*, Performance of the LHCb vertex locator, *J. Instrum.* **9**, P09007 (2014).
- [51] R. Aaij *et al.* (LHCb Collaboration), Precision measurement of the $B_s^0-\bar{B}_s^0$ oscillation frequency in the decay $B_s^0 \rightarrow D_s^-\pi^+$, *New J. Phys.* **15**, 053021 (2013).
- [52] M. Needham (LHCb Collaboration), Momentum scale calibration using resonances, Report No. CERN-LHCb-2008-037, 2008, http://cdsweb.cern.ch/search?p=CERN-LHCb-2008-037&f=reportnumber&action_search=Search&c=LHCb.

Correction: A typographical error in the value of $\Gamma_s - \Gamma_d$ in the third sentence of the abstract has been fixed.

- R. Aaij¹,³³ A. S. W. Abdelmotteleb¹,⁵² C. Abellan Beteta,⁴⁶ F. Abudinén¹,⁵² T. Ackernley¹,⁵⁶ B. Adeva¹,⁴² M. Adinolfi¹,⁵⁰ P. Adlarson¹,⁷⁸ H. Afsharnia,¹⁰ C. Agapopoulou¹,⁴⁴ C. A. Aidala¹,⁷⁹ Z. Ajaltouni,¹⁰ S. Akar¹,⁶¹ K. Akiba¹,³³ P. Albicocco¹,²⁴ J. Albrecht¹,¹⁶ F. Alessio¹,⁴⁴ M. Alexander¹,⁵⁵ A. Alfonso Albero¹,⁴¹ Z. Aliouche¹,⁵⁸ P. Alvarez Cartelle¹,⁵¹ R. Amalric¹,¹⁴ S. Amato¹,² J. L. Amey¹,⁵⁰ Y. Amhis¹,^{12,44} L. An¹,⁵ L. Anderlini¹,²³ M. Andersson¹,⁴⁶ A. Andreianov¹,³⁹ P. Andreola¹,⁴⁶ M. Andreotti¹,²² D. Andreou¹,⁶⁴ D. Ao¹,⁶ F. Archilli¹,^{32,b} A. Artamonov¹,³⁹ M. Artuso¹,⁶⁴ E. Aslanides¹,¹¹ M. Atzeni¹,⁶⁰ B. Audurier¹,¹³ D. Bacher¹,⁵⁹ I. Bachiller Perea¹,⁹ S. Bachmann¹,¹⁸ M. Bachmayer¹,⁴⁵ J. J. Back¹,⁵² A. Bailly-reyre,¹⁴ P. Baladron Rodriguez¹,⁴² V. Balagura¹,¹³ W. Baldini¹,^{22,44} J. Baptista de Souza Leite¹,¹ M. Barbetti¹,^{23,c} I. R. Barbosa¹,⁶⁶ R. J. Barlow¹,⁵⁸ S. Barsuk¹,¹² W. Barter¹,⁵⁴ M. Bartolini¹,⁵¹ F. Baryshnikov¹,³⁹ J. M. Basels¹,¹⁵ G. Bassi¹,^{30,d} B. Batsukh¹,⁴ A. Battig¹,¹⁶ A. Bay¹,⁴⁵ A. Beck¹,⁵² M. Becker¹,¹⁶ F. Bedeschi¹,³⁰ I. B. Bediaga¹,¹ A. Beiter¹,⁶⁴ S. Belin¹,⁴² V. Bellee¹,⁴⁶ K. Belous¹,³⁹ I. Belov¹,²⁵ I. Belyaev¹,³⁹ G. Benane¹,¹¹ G. Bencivenni¹,²⁴ E. Ben-Haim¹,¹⁴ A. Berezhnoy¹,³⁹ R. Bernet¹,⁴⁶ S. Bernet Andres¹,⁴⁰ D. Berninghoff¹,¹⁸ H. C. Bernstein,⁶⁴ C. Bertella¹,⁵⁸ A. Bertolin¹,²⁹ C. Betancourt¹,⁴⁶ F. Betti¹,⁵⁴ J. Bex¹,⁵¹ Ia. Bezshyiko¹,⁴⁶ J. Bhom¹,³⁶ L. Bian¹,⁷⁰ M. S. Bieker¹,¹⁶ N. V. Biesuz¹,²² P. Billoir¹,¹⁴ A. Biolchini¹,³³ M. Birch¹,⁵⁷ F. C. R. Bishop¹,⁵¹ A. Bitadze¹,⁵⁸ A. Bizzeti¹,¹ M. P. Blago¹,⁵¹ T. Blake¹,⁵² F. Blanc¹,⁴⁵ J. E. Blank¹,¹⁶ S. Blusk¹,⁶⁴ D. Bobulska¹,⁵⁵ V. Bocharnikov¹,³⁹ J. A. Boelhauve¹,¹⁶ O. Boente Garcia¹,¹³ T. Boettcher¹,⁶¹ A. Bohare¹,⁵⁴ A. Boldyrev¹,³⁹ C. S. Bolognani¹,⁷⁶ R. Bolzonella¹,^{22,e} N. Bondar¹,³⁹ F. Borgato¹,^{29,44} S. Borghi¹,⁵⁸ M. Borsato¹,¹⁸ J. T. Borsuk¹,³⁶ S. A. Bouchiba¹,⁴⁵ T. J. V. Bowcock¹,⁵⁶ A. Boyer¹,⁴⁴ C. Bozzi¹,²² M. J. Bradley,⁵⁷ S. Braun¹,⁶² A. Brea Rodriguez¹,⁴² N. Breer¹,¹⁶ J. Brodzicka¹,³⁶ A. Brossa Gonzalo¹,⁴² J. Brown¹,⁵⁶ D. Brundu¹,²⁸ A. Buonaaura¹,⁴⁶ L. Buonincontri¹,²⁹ A. T. Burke¹,⁵⁸ C. Burr¹,⁴⁴ A. Bursche,⁶⁸ A. Butkevich¹,³⁹ J. S. Butter¹,³³ J. Buytaert¹,⁴⁴ W. Byczynski¹,⁴⁴ S. Cadeddu¹,²⁸ H. Cai,⁷⁰ R. Calabrese¹,^{22,e} L. Calefice¹,¹⁶ S. Cali¹,²⁴ M. Calvi¹,^{27,f} M. Calvo Gomez¹,⁴⁰ J. Cambon Bouzas¹,⁴² P. Campana¹,²⁴ D. H. Campora Perez¹,⁷⁶ A. F. Campoverde Quezada¹,⁶ S. Capelli¹,^{27,f} L. Capriotti¹,²² A. Carbone¹,^{21,g} L. Carcedo Salgado¹,⁴² R. Cardinale¹,^{25,h} A. Cardini¹,²⁸ P. Carniti¹,^{27,f} L. Carus,¹⁸ A. Casais Vidal¹,⁴² R. Caspary¹,¹⁸ G. Casse¹,⁵⁶ M. Cattaneo¹,⁴⁴ G. Cavallero¹,²² V. Cavallini¹,^{22,e} S. Celani¹,⁴⁵ J. Cerasoli¹,¹¹ D. Cervenkov¹,⁵⁹ A. J. Chadwick¹,⁵⁶ I. Chahroud¹,⁷⁹ M. G. Chapman,⁵⁰ M. Charles¹,¹⁴ Ph. Charpentier¹,⁴⁴ C. A. Chavez Barajas¹,⁵⁶ M. Chefdeville¹,⁹ C. Chen¹,¹¹ S. Chen¹,⁴ A. Chernov¹,³⁶ S. Chernyshenko¹,⁴⁸ V. Chobanova¹,^{42,i} S. Cholak¹,⁴⁵ M. Chrzaszcz¹,³⁶ A. Chubykin¹,³⁹ V. Chulikov¹,³⁹ P. Ciambrone¹,²⁴ M. F. Cicala¹,⁵² X. Cid Vidal¹,⁴² G. Ciezarek¹,⁴⁴ P. Cifra¹,⁴⁴ P. E. L. Clarke¹,⁵⁴ M. Clemencic¹,⁴⁴

- H. V. Cliff⁵¹, J. Closier⁴⁴, J. L. Cobbledick⁵⁸, C. Cocha Toapaxi¹⁸, V. Coco⁴⁴, J. Cogan¹¹, E. Cogneras¹⁰, L. Cojocariu³⁸, P. Collins⁴⁴, T. Colombo⁴⁴, A. Comerma-Montells⁴¹, L. Congedo²⁰, A. Contu²⁸, N. Cooke⁵⁵, I. Corredoira⁴², A. Correia¹⁴, G. Corti⁴⁴, J. J. Cottee Meldrum⁵⁰, B. Couturier⁴⁴, D. C. Craik⁴⁶, M. Cruz Torres^{1,j}, R. Currie⁵⁴, C. L. Da Silva⁶³, S. Dadabaev³⁹, L. Dai⁶⁷, X. Dai⁵, E. Dall'Occo¹⁶, J. Dalseno⁴², C. D'Ambrosio⁴⁴, J. Daniel¹⁰, A. Danilina³⁹, P. d'Argent²⁰, A. Davidson⁵², J. E. Davies⁵⁸, A. Davis⁵⁸, O. De Aguiar Francisco⁵⁸, J. de Boer³³, K. De Bruyn⁷⁵, S. De Capua⁵⁸, M. De Cian¹⁸, U. De Freitas Carneiro Da Graca^{1,k}, E. De Lucia²⁴, J. M. De Miranda¹, L. De Paula², M. De Serio^{20,l}, D. De Simone⁴⁶, P. De Simone²⁴, F. De Vellis¹⁶, J. A. de Vries⁷⁶, C. T. Dean⁶³, F. Debernardis^{20,l}, D. Decamp⁹, V. Dedu¹¹, L. Del Buono¹⁴, B. Delaney⁶⁰, H.-P. Dembinski¹⁶, V. Denysenko⁴⁶, O. Deschamps¹⁰, F. Dettori^{28,m}, B. Dey⁷³, P. Di Nezza²⁴, I. Diachkov³⁹, S. Didenko³⁹, S. Ding⁶⁴, V. Dobishuk⁴⁸, A. D. Docheva⁵⁵, A. Dolmatov³⁹, C. Dong³, A. M. Donohoe¹⁹, F. Dordei²⁸, A. C. dos Reis¹, L. Douglas⁵⁵, A. G. Downes⁹, W. Duan⁶⁸, P. Duda⁷⁷, M. W. Dudek³⁶, L. Dufour⁴⁴, V. Duk⁷⁴, P. Durante⁴⁴, M. M. Duras⁷⁷, J. M. Durham⁶³, D. Dutta⁵⁸, A. Dziurda³⁶, A. Dzyuba³⁹, S. Easo^{53,44}, E. Eckstein⁷², U. Egede⁶⁵, A. Egorychev³⁹, V. Egorychev³⁹, C. Eirea Orro⁴², S. Eisenhardt⁵⁴, E. Ejopu⁵⁸, S. Ek-In⁴⁵, L. Eklund⁷⁸, M. Elashri⁶¹, J. Ellbracht¹⁶, S. Ely⁵⁷, A. Ene³⁸, E. Epple⁶¹, S. Escher¹⁵, J. Eschle⁴⁶, S. Esen⁴⁶, T. Evans⁵⁸, F. Fabiano^{28,44,m}, L. N. Falcao¹, Y. Fan⁶, B. Fang^{70,12}, L. Fantini^{74,n}, M. Faria⁴⁵, K. Farmer⁵⁴, S. Farry⁵⁶, D. Fazzini^{27,f}, L. Felkowski⁷⁷, M. Feng⁴⁶, M. Feo⁴⁴, M. Fernandez Gomez⁴², A. D. Fernez⁶², F. Ferrari²¹, L. Ferreira Lopes⁴⁵, F. Ferreira Rodrigues², S. Ferreres Sole³³, M. Ferrillo⁴⁶, M. Ferro-Luzzi⁴⁴, S. Filippov³⁹, R. A. Fini²⁰, M. Fiorini^{22,e}, M. Firlej³⁵, K. M. Fischer⁵⁹, D. S. Fitzgerald⁷⁹, C. Fitzpatrick⁵⁸, T. Fiutowski³⁵, F. Fleuret¹³, M. Fontana²¹, F. Fontanelli^{25,h}, L. F. Foreman⁵⁸, R. Forty⁴⁴, D. Foulds-Holt⁵¹, M. Franco Sevilla⁶², M. Frank⁴⁴, E. Franzoso^{22,e}, G. Frau¹⁸, C. Frei⁴⁴, D. A. Friday⁵⁸, L. Frontini^{26,o}, J. Fu⁶, Q. Fuehring¹⁶, Y. Fujii⁶⁵, T. Fulghesu¹⁴, E. Gabriel³³, G. Galati^{20,l}, M. D. Galati³³, A. Gallas Torreira⁴², D. Galli^{21,g}, S. Gambetta^{54,44}, M. Gandelman², P. Gandini²⁶, H. Gao⁶, R. Gao⁵⁹, Y. Gao⁷, Y. Gao⁵, M. Garau^{28,m}, L. M. Garcia Martin⁴⁵, P. Garcia Moreno⁴¹, J. Garcia Pardiñas⁴⁴, B. Garcia Plana⁴², F. A. Garcia Rosales¹³, L. Garrido⁴¹, C. Gaspar⁴⁴, R. E. Geertsema³³, L. L. Gerken¹⁶, E. Gersabeck⁵⁸, M. Gersabeck⁵⁸, T. Gershon⁵², L. Giambastiani²⁹, F. I. Giasemis^{14,p}, V. Gibson⁵¹, H. K. Giemza³⁷, A. L. Gilman⁵⁹, M. Giovannetti²⁴, A. Gioventù⁴², P. Gironella Gironell⁴¹, C. Giugliano^{22,e}, M. A. Giza³⁶, K. Gizdov⁵⁴, E. L. Gkougkousis⁴⁴, F. C. Glaser^{12,18}, V. V. Gligorov¹⁴, C. Göbel⁶⁶, E. Golobardes⁴⁰, D. Golubkov³⁹, A. Golutvin^{57,39,44}, A. Gomes^{1,1,2,a,q,r,q}, S. Gomez Fernandez⁴¹, F. Goncalves Abrantes⁵⁹, M. Goncerz³⁶, G. Gong³, J. A. Gooding¹⁶, I. V. Gorelov³⁹, C. Gotti²⁷, J. P. Grabowski⁷², L. A. Granado Cardoso⁴⁴, E. Graugés⁴¹, E. Graverini⁴⁵, L. Grazette⁵², G. Graziani¹, A. T. Grecu³⁸, L. M. Greeven³³, N. A. Grieser⁶¹, L. Grillo⁵⁵, S. Gromov³⁹, C. Gu¹³, M. Guarise²², M. Guittiere¹², V. Guliaeva³⁹, P. A. Günther¹⁸, A. K. Guseinov³⁹, E. Gushchin³⁹, Y. Guz^{5,39,44}, T. Gys⁴⁴, T. Hadavizadeh⁶⁵, C. Hadjivasilou⁶², G. Haefeli⁴⁵, C. Haen⁴⁴, J. Haimberger⁴⁴, S. C. Haines⁵¹, M. Hajheidari⁴⁴, T. Halewood-leagas⁵⁶, M. M. Halvorsen⁴⁴, P. M. Hamilton⁶², J. Hammerich⁵⁶, Q. Han⁷, X. Han¹⁸, S. Hansmann-Menzemer¹⁸, L. Hao⁶, N. Harnew⁵⁹, T. Harrison⁵⁶, M. Hartmann¹², C. Hasse⁴⁴, M. Hatch⁴⁴, J. He^{6,s}, K. Heijhoff³³, F. Hemmer⁴⁴, C. Henderson⁶¹, R. D. L. Henderson^{65,52}, A. M. Hennequin⁴⁴, K. Hennessy⁵⁶, L. Henry⁴⁵, J. Herd⁵⁷, J. Heuel¹⁵, A. Hicheur², D. Hill⁴⁵, M. Hilton⁵⁸, S. E. Hollitt¹⁶, J. Horswill⁵⁸, R. Hou⁷, Y. Hou⁹, N. Howarth⁵⁶, J. Hu¹⁸, J. Hu⁶⁸, W. Hu⁵, X. Hu³, W. Huang⁶, X. Huang⁷⁰, W. Hulsbergen³³, R. J. Hunter⁵², M. Hushchyn³⁹, D. Hutchcroft⁵⁶, P. Ibis¹⁶, M. Idzik³⁵, D. Ilin³⁹, P. Ilten⁶¹, A. Inglessi³⁹, A. Iniuikhin³⁹, A. Ishteev³⁹, K. Ivshin³⁹, R. Jacobsson⁴⁴, H. Jage¹⁵, S. J. Jaimes Elles^{43,71}, S. Jakobsen⁴⁴, E. Jans³³, B. K. Jashal⁴³, A. Jawahery⁶², V. Jevtic¹⁶, E. Jiang⁶², X. Jiang^{4,6}, Y. Jiang⁶, Y. J. Jiang⁵, M. John⁵⁹, D. Johnson⁴⁹, C. R. Jones⁵¹, T. P. Jones⁵², S. Joshi³⁷, B. Jost⁴⁴, N. Jurik⁴⁴, I. Juszczak³⁶, D. Kaminaris⁴⁵, S. Kandybei⁴⁷, Y. Kang³, M. Karacson⁴⁴, D. Karpenkov³⁹, M. Karpov³⁹, A. M. Kauniskangas⁴⁵, J. W. Kautz⁶¹, F. Keizer⁴⁴, D. M. Keller⁶⁴, M. Kenzie⁵¹, T. Ketel³³, B. Khanji⁶⁴, A. Kharisova³⁹, S. Kholodenko³⁰, G. Khreich¹², T. Kirn¹⁵, V. S. Kirsebom⁴⁵, O. Kitouni⁶⁰, S. Klaver³⁴, N. Kleijne^{30,d}, K. Klimaszewski³⁷, M. R. Kmiec³⁷, S. Kolliiev⁴⁸, L. Kolk¹⁶, A. Konoplyannikov³⁹, P. Kopciewicz^{35,44}, R. Kopecna¹⁸, P. Koppenburg³³, M. Korolev³⁹, I. Kostiuk³³, O. Kot⁴⁸, S. Kotriakhova⁴⁰, A. Kozachuk³⁹, P. Kravchenko³⁹, L. Kravchuk³⁹, M. Kreps⁵², S. Kretzschmar¹⁵, P. Krokovny³⁹, W. Krupa⁶⁴, W. Krzemien³⁷, J. Kubat¹⁸, S. Kubis⁷⁷, W. Kucewicz³⁶, M. Kucharczyk³⁶, V. Kudryavtsev³⁹, E. Kulikova³⁹

- A. Kupsc¹,⁷⁸ B. K. Kutsenko¹,¹¹ D. Lacarrere¹,⁴⁴ G. Lafferty¹,⁵⁸ A. Lai¹,²⁸ A. Lampis¹,^{28,m} D. Lancierini¹,⁴⁶ C. Landesa Gomez¹,⁴² J. J. Lane¹,⁶⁵ R. Lane¹,⁵⁰ C. Langenbruch¹,¹⁸ J. Langer¹,¹⁶ O. Lantwin¹,³⁹ T. Latham¹,⁵² F. Lazzari¹,^{30,t} C. Lazzeroni¹,⁴⁹ R. Le Gac¹,¹¹ S. H. Lee¹,⁷⁹ R. Lefèvre¹,¹⁰ A. Leflat¹,³⁹ S. Legotin¹,³⁹ O. Leroy¹,¹¹ T. Lesiak¹,³⁶ B. Leverington¹,¹⁸ A. Li¹,³ H. Li¹,⁶⁸ K. Li¹,⁷ L. Li¹,⁵⁸ P. Li¹,⁴⁴ P.-R. Li¹,⁶⁹ S. Li¹,⁷ T. Li¹,⁴ T. Li¹,⁶⁸ Y. Li¹,⁴ Z. Li¹,⁶⁴ Z. Lian¹,³ X. Liang¹,⁶⁴ C. Lin¹,⁶ T. Lin¹,⁵³ R. Lindner¹,⁴⁴ V. Lisovskyi¹,⁴⁵ R. Litvinov¹,^{28,m} G. Liu¹,⁶⁸ H. Liu¹,⁶ K. Liu¹,⁶⁹ Q. Liu¹,⁶ S. Liu¹,^{4,6} Y. Liu¹,⁵⁴ Y. Liu¹,⁶⁹ A. Lobo Salvia¹,⁴¹ A. Loi¹,²⁸ J. Lomba Castro¹,⁴² T. Long¹,⁵¹ I. Longstaff¹,⁵⁵ J. H. Lopes¹,² A. Lopez Huertas¹,⁴¹ S. López Soliño¹,⁴² G. H. Lovell¹,⁵¹ Y. Lu¹,^{4,u} C. Lucarelli¹,^{23,c} D. Lucchesi¹,^{29,v} S. Luchuk¹,³⁹ M. Lucio Martinez¹,⁷⁶ V. Lukashenko¹,^{33,48} Y. Luo¹,³ A. Lupato¹,²⁹ E. Luppi¹,^{22,e} K. Lynch¹,¹⁹ X.-R. Lyu¹,⁶ R. Ma¹,⁶ S. Maccolini¹,¹⁶ F. Machefert¹,¹² F. Maciuc¹,³⁸ I. Mackay¹,⁵⁹ L. R. Madhan Mohan¹,⁵¹ M. M. Madurai¹,⁴⁹ A. Maevskiy¹,³⁹ D. Magdalinski¹,³³ D. Maisuzenko¹,³⁹ M. W. Majewski¹,³⁵ J. J. Malczewski¹,³⁶ S. Malde¹,⁵⁹ B. Malecki¹,^{36,44} L. Malentacca¹,⁴⁴ A. Malinin¹,³⁹ T. Maltsev¹,³⁹ G. Manca¹,^{28,m} G. Mancinelli¹,¹¹ C. Mancuso¹,^{26,12,o} R. Manera Escalero¹,⁴¹ D. Manuzzi¹,²¹ C. A. Manzari¹,⁴⁶ D. Marangotto¹,^{26,o} J. F. Marchand¹,⁹ U. Marconi¹,²¹ S. Mariani¹,⁴⁴ C. Marin Benito¹,^{41,44} J. Marks¹,¹⁸ A. M. Marshall¹,⁵⁰ P. J. Marshall¹,⁵⁶ G. Martelli¹,^{74,n} G. Martellotti¹,³¹ L. Martinazzoli¹,⁴⁴ M. Martinelli¹,^{27,f} D. Martinez Santos¹,⁴² F. Martinez Vidal¹,⁴³ A. Massafferri¹,¹ M. Materok¹,¹⁵ R. Matev¹,⁴⁴ A. Mathad¹,⁴⁶ V. Matiunin¹,³⁹ C. Matteuzzi¹,^{64,27} K. R. Mattioli¹,¹³ A. Mauri¹,⁵⁷ E. Maurice¹,¹³ J. Mauricio¹,⁴¹ M. Mazurek¹,⁴⁴ M. McCann¹,⁵⁷ L. Mcconnell¹,¹⁹ T. H. McGrath¹,⁵⁸ N. T. McHugh¹,⁵⁵ A. McNab¹,⁵⁸ R. McNulty¹,¹⁹ B. Meadows¹,⁶¹ G. Meier¹,¹⁶ D. Melnychuk¹,³⁷ M. Merk¹,^{33,76} A. Merli¹,^{26,o} L. Meyer Garcia¹,² D. Miao¹,^{4,6} H. Miao¹,⁶ M. Mikhasenko¹,^{72,w} D. A. Milanes¹,⁷¹ M.-N. Minard¹,^{9,a} A. Minotti¹,^{27,f} E. Minucci¹,⁶⁴ T. Miralles¹,¹⁰ S. E. Mitchell¹,⁵⁴ B. Mitreska¹,¹⁶ D. S. Mitzel¹,¹⁶ A. Modak¹,⁵³ A. Mödden¹,¹⁶ R. A. Mohammed¹,⁵⁹ R. D. Moise¹,¹⁵ S. Mokhnenko¹,³⁹ T. Mombächer¹,⁴⁴ M. Monk¹,^{52,65} I. A. Monroy¹,⁷¹ S. Monteil¹,¹⁰ A. Morcillo Gomez¹,⁴² G. Morello¹,²⁴ M. J. Morello¹,^{30,d} M. P. Morgenthaler¹,¹⁸ J. Moron¹,³⁵ A. B. Morris¹,⁴⁴ A. G. Morris¹,¹¹ R. Mountain¹,⁶⁴ H. Mu¹,³ Z. M. Mu¹,⁵ E. Muhammad¹,⁵² F. Muheim¹,⁵⁴ M. Mulder¹,⁷⁵ K. Müller¹,⁴⁶ F. Múnoz-Rojas¹,⁸ R. Murta¹,⁵⁷ P. Naik¹,⁴⁵ T. Nakada¹,⁴⁵ R. Nandakumar¹,⁵³ T. Nanut¹,⁴⁴ I. Nasteva¹,² M. Needham¹,⁵⁴ N. Neri¹,^{26,o} S. Neubert¹,⁷² N. Neufeld¹,⁴⁴ P. Neustroev¹,³⁹ R. Newcombe¹,⁵⁷ J. Nicolini¹,^{16,12} D. Nicotra¹,⁷⁶ E. M. Niel¹,⁴⁵ N. Nikitin¹,³⁹ P. Nogga¹,⁷² N. S. Nolte¹,⁶⁰ C. Normand¹,^{9,28,m} J. Novoa Fernandez¹,⁴² G. Nowak¹,⁶¹ C. Nunez¹,⁷⁹ H. N. Nur¹,⁵⁵ A. Oblakowska-Mucha¹,³⁵ V. Obraztsov¹,³⁹ T. Oeser¹,¹⁵ S. Okamura¹,^{22,44,e} R. Oldeman¹,^{28,m} F. Oliva¹,⁵⁴ M. Olocco¹,¹⁶ C. J. G. Onderwater¹,⁷⁶ R. H. O'Neil¹,⁵⁴ J. M. Otalora Goicochea¹,² T. Ovsiannikova¹,³⁹ P. Owen¹,⁴⁶ A. Oyanguren¹,⁴³ O. Ozcelik¹,⁵⁴ K. O. Padeken¹,⁷² B. Pagare¹,⁵² P. R. Pais¹,¹⁸ T. Pajero¹,⁵⁹ A. Palano¹,²⁰ M. Palutan¹,²⁴ G. Panshin¹,³⁹ L. Paolucci¹,⁵² A. Papanestis¹,⁵³ M. Pappagallo¹,^{20,l} L. L. Pappalardo¹,^{22,e} C. Pappenheimer¹,⁶¹ C. Parkes¹,^{58,44} B. Passalacqua¹,^{22,e} G. Passaleva¹,²³ D. Passaro¹,³⁰ A. Pastore¹,²⁰ M. Patel¹,⁵⁷ J. Patoc¹,⁵⁹ C. Patrignani¹,^{21,g} C. J. Pawley¹,⁷⁶ A. Pellegrino¹,³³ M. Pepe Altarelli¹,²⁴ S. Perazzini¹,²¹ D. Pereima¹,³⁹ A. Pereiro Castro¹,⁴² P. Perret¹,¹⁰ A. Perro¹,⁴⁴ K. Petridis¹,⁵⁰ A. Petrolini¹,^{25,h} S. Petrucci¹,⁵⁴ H. Pham¹,⁶⁴ A. Philippov¹,³⁹ L. Pica¹,^{30,d} M. Piccini¹,⁷⁴ B. Pietrzyk¹,⁹ G. Pietrzyk¹,¹² D. Pinci¹,³¹ F. Pisani¹,⁴⁴ M. Pizzichemi¹,^{27,f} V. Placinta¹,³⁸ M. Plo Casasus¹,⁴² F. Polci¹,^{14,44} M. Poli Lener¹,²⁴ A. Poluektov¹,¹¹ N. Polukhina¹,³⁹ I. Polyakov¹,⁴⁴ E. Polycarpo¹,² S. Ponce¹,⁴⁴ D. Popov¹,⁶ S. Poslavskii¹,³⁹ K. Prasanth¹,³⁶ L. Promberger¹,¹⁸ C. Prouve¹,⁴² V. Pugatch¹,⁴⁸ V. Puill¹,¹² G. Punzi¹,^{30,t} H. R. Qi¹,³ W. Qian¹,⁶ N. Qin¹,³ S. Qu¹,³ R. Quagliani¹,⁴⁵ B. Rachwal¹,³⁵ J. H. Rademacker¹,⁵⁰ M. Rama¹,³⁰ M. Ramírez García¹,⁷⁹ M. Ramos Pernas¹,⁵² M. S. Rangel¹,² F. Ratnikov¹,³⁹ G. Raven¹,³⁴ M. Rebollo De Miguel¹,⁴³ F. Redi¹,⁴⁴ J. Reich¹,⁵⁰ F. Reiss¹,⁵⁸ Z. Ren¹,³ P. K. Resmi¹,⁵⁹ R. Ribatti¹,^{30,d} G. R. Ricart¹,^{13,80} D. Riccardi¹,³⁰ S. Ricciardi¹,⁵³ K. Richardson¹,⁶⁰ M. Richardson-Slipper¹,⁵⁴ K. Rinnert¹,⁵⁶ P. Robbe¹,¹² G. Robertson¹,⁵⁴ E. Rodrigues¹,^{56,44} E. Rodriguez Fernandez¹,⁴² J. A. Rodriguez Lopez¹,⁷¹ E. Rodriguez Rodriguez¹,⁴² A. Rogovskiy¹,⁵³ D. L. Rolf¹,⁴⁴ A. Rollings¹,⁵⁹ P. Roloff¹,⁴⁴ V. Romanovskiy¹,³⁹ M. Romero Lamas¹,⁴² A. Romero Vidal¹,⁴² G. Romolini¹,²² F. Ronchetti¹,⁴⁵ M. Rotondo¹,²⁴ M. S. Rudolph¹,⁶⁴ T. Ruf¹,⁴⁴ R. A. Ruiz Fernandez¹,⁴² J. Ruiz Vidal¹,⁴³ A. Ryzhikov¹,³⁹ J. Ryzka¹,³⁵ J. J. Saborido Silva¹,⁴² N. Sagidova¹,³⁹ N. Sahoo¹,⁴⁹ B. Saitta¹,^{28,m} M. Salomoni¹,⁴⁴ C. Sanchez Gras¹,³³ I. Sanderswood¹,⁴³ R. Santacesaria¹,³¹ C. Santamarina Rios¹,⁴² M. Santimaria¹,²⁴ L. Santoro¹,¹ E. Santovetti¹,³² D. Saranin¹,³⁹ G. Sarpis¹,⁵⁴ M. Sarpis¹,⁷² A. Sarti¹,³¹ C. Satriano¹,^{31,x} A. Satta¹,³² M. Sauri¹,⁵ D. Savrina¹,³⁹ H. Sazak¹,¹⁰ L. G. Scantlebury Smead¹,⁵⁹ A. Scarabotto¹,¹⁴ S. Schael¹,¹⁵ S. Scherl¹,⁵⁶ A. M. Schertz¹,⁷³ M. Schiller¹,⁵⁵ H. Schindler¹,⁴⁴ M. Schmelling¹,¹⁷ B. Schmidt¹,⁴⁴ S. Schmitt¹,¹⁵ O. Schneider¹,⁴⁵ A. Schopper¹,⁴⁴

- N. Schulte¹⁶, S. Schulte⁴⁵, M. H. Schune¹², R. Schwemmer⁴⁴, G. Schwering¹⁵, B. Sciascia²⁴, A. Sciuccati⁴⁴, S. Sellam⁴², A. Semennikov³⁹, M. Senghi Soares³⁴, A. Sergi^{25,h}, N. Serra^{46,44}, L. Sestini²⁹, A. Seuthe¹⁶, Y. Shang⁵, D. M. Shangase⁷⁹, M. Shapkin³⁹, I. Shchemberov³⁹, L. Shchutska⁴⁵, T. Shears⁵⁶, L. Shekhtman³⁹, Z. Shen⁵, S. Sheng^{4,6}, V. Shevchenko³⁹, B. Shi⁶, E. B. Shields^{27,f}, Y. Shimizu¹², E. Shmanin³⁹, R. Shorkin³⁹, J. D. Shupperd⁶⁴, B. G. Siddi^{22,e}, R. Silva Coutinho⁶⁴, G. Simi²⁹, S. Simone^{20,l}, M. Singla⁶⁵, N. Skidmore⁵⁸, R. Skuza¹⁸, T. Skwarnicki⁶⁴, M. W. Slater⁴⁹, J. C. Smallwood⁵⁹, J. G. Smeaton⁵¹, E. Smith⁶⁰, K. Smith⁶³, M. Smith⁵⁷, A. Snoch³³, L. Soares Lavra⁵⁴, M. D. Sokoloff⁶¹, F. J. P. Soler⁵⁵, A. Solomin^{39,50}, A. Solovev³⁹, I. Solovyev³⁹, R. Song⁶⁵, Y. Song⁴⁵, Y. Song³, Y. S. Song⁵, F. L. Souza De Almeida², B. Souza De Paula², E. Spadaro Norella^{26,o}, E. Spedicato²¹, J. G. Speer¹⁶, E. Spiridenkov³⁹, P. Spradlin⁵⁵, V. Sriskaran⁴⁴, F. Stagni⁴⁴, M. Stahl⁴⁴, S. Stahl⁴⁴, S. Stanislaus⁵⁹, E. N. Stein⁴⁴, O. Steinkamp⁴⁶, O. Stenyakin³⁹, H. Stevens¹⁶, D. Strekalina³⁹, Y. Su⁶, F. Suljik⁵⁹, J. Sun²⁸, L. Sun⁷⁰, Y. Sun⁶², P. N. Swallow⁴⁹, K. Swientek³⁵, F. Swystun⁵², A. Szabelski³⁷, T. Szumlak³⁵, M. Szymanski⁴⁴, Y. Tan³, S. Taneja⁵⁸, M. D. Tat⁵⁹, A. Terentev⁴⁶, F. Teubert⁴⁴, E. Thomas⁴⁴, D. J. D. Thompson⁴⁹, H. Tilquin⁵⁷, V. Tisserand¹⁰, S. T'Jampens⁹, M. Tobin⁴, L. Tomassetti^{22,e}, G. Tonani^{26,o}, X. Tong⁵, D. Torres Machado¹, L. Toscano¹⁶, D. Y. Tou³, C. Trippel⁴⁵, G. Tuci¹⁸, N. Tuning³³, A. Ukleja³⁷, D. J. Unverzagt¹⁸, E. Ursov³⁹, A. Usachov³⁴, A. Ustyuzhanin³⁹, U. Uwer¹⁸, V. Vagnoni²¹, A. Valassi⁴⁴, G. Valenti²¹, N. Valls Canudas⁴⁰, M. Van Dijk⁴⁵, H. Van Hecke⁶³, E. van Herwijnen⁵⁷, C. B. Van Hulse^{42,y}, R. Van Laak⁴⁵, M. van Veghel³³, R. Vazquez Gomez⁴¹, P. Vazquez Regueiro⁴², C. Vázquez Sierra⁴², S. Vecchi²², J. J. Velthuis⁵⁰, M. Veltri^{23,z}, A. Venkateswaran⁴⁵, M. Vesterinen⁵², D. Vieira⁶¹, M. Vieites Diaz⁴⁴, X. Vilasis-Cardona⁴⁰, E. Vilella Figueras⁵⁶, A. Villa²¹, P. Vincent¹⁴, F. C. Volle¹², D. vom Bruch¹¹, V. Vorobyev³⁹, N. Voropaev³⁹, K. Vos⁷⁶, C. Vrahas⁵⁴, J. Walsh³⁰, E. J. Walton⁶⁵, G. Wan⁵, C. Wang¹⁸, G. Wang⁷, J. Wang⁵, J. Wang⁴, J. Wang³, J. Wang⁷⁰, M. Wang²⁶, N. W. Wang⁶, R. Wang⁵⁰, X. Wang⁶⁸, Y. Wang⁷, Z. Wang⁴⁶, Z. Wang³, Z. Wang⁶, J. A. Ward^{52,65}, N. K. Watson⁴⁹, D. Websdale⁵⁷, Y. Wei⁵, B. D. C. Westhenry⁵⁰, D. J. White⁵⁸, M. Whitehead⁵⁵, A. R. Wiederhold⁵², D. Wiedner¹⁶, G. Wilkinson⁵⁹, M. K. Wilkinson⁶¹, I. Williams⁵¹, M. Williams⁶⁰, M. R. J. Williams⁵⁴, R. Williams⁵¹, F. F. Wilson⁵³, W. Wislicki³⁷, M. Witek³⁶, L. Witola¹⁸, C. P. Wong⁶³, G. Wormser¹², S. A. Wotton⁵¹, H. Wu⁶⁴, J. Wu⁷, Y. Wu⁵, K. Wyllie⁴⁴, S. Xian⁶⁸, Z. Xiang⁴, Y. Xie⁷, A. Xu³⁰, J. Xu⁶, L. Xu³, L. Xu³, M. Xu⁵², Z. Xu¹⁰, Z. Xu⁶, Z. Xu⁴, D. Yang³, S. Yang⁶, X. Yang⁵, Y. Yang²⁵, Z. Yang⁵, Z. Yang⁶², V. Yeroshenko¹², H. Yeung⁵⁸, H. Yin⁷, C. Y. Yu⁵, J. Yu⁶⁷, X. Yuan⁴, E. Zaffaroni⁴⁵, M. Zavertyaev¹⁷, M. Zdybal³⁶, M. Zeng³, C. Zhang⁵, D. Zhang⁷, J. Zhang⁶, L. Zhang³, S. Zhang⁶⁷, S. Zhang⁵, Y. Zhang⁵, Y. Zhang⁵⁹, Y. Zhao¹⁸, A. Zharkova³⁹, A. Zhelezov¹⁸, Y. Zheng⁶, T. Zhou⁵, X. Zhou⁷, Y. Zhou⁶, V. Zhovkovska¹², L. Z. Zhu⁶, X. Zhu³, X. Zhu⁷, Z. Zhu⁶, V. Zhukov^{15,39}, J. Zhuo⁴³, Q. Zou^{4,6}, S. Zucchelli^{21,g}, D. Zuliani²⁹, and G. Zunic⁵⁸

(LHCb Collaboration)

¹Centro Brasileiro de Pesquisas Físicas (CBPF), Rio de Janeiro, Brazil²Universidade Federal do Rio de Janeiro (UFRJ), Rio de Janeiro, Brazil³Center for High Energy Physics, Tsinghua University, Beijing, China⁴Institute of High Energy Physics (IHEP), Beijing, China⁵School of Physics State Key Laboratory of Nuclear Physics and Technology, Peking University, Beijing, China⁶University of Chinese Academy of Sciences, Beijing, China⁷Institute of Particle Physics, Central China Normal University, Wuhan, Hubei, China⁸Consejo Nacional de Rectores (CONARE), San Jose, Costa Rica⁹Université Savoie Mont Blanc, CNRS/IN2P3-LAPP, Annecy, France¹⁰Université Clermont Auvergne, CNRS/IN2P3, LPC, Clermont-Ferrand, France¹¹Aix Marseille Univ, CNRS/IN2P3, CPPM, Marseille, France¹²Université Paris-Saclay, CNRS/IN2P3, IJCLab, Orsay, France¹³Laboratoire Leprince-Ringuet, CNRS/IN2P3, Ecole Polytechnique, Institut Polytechnique de Paris, Palaiseau, France¹⁴LPNHE, Sorbonne Université, Paris Diderot Sorbonne Paris Cité, CNRS/IN2P3, Paris, France¹⁵I. Physikalisches Institut, RWTH Aachen University, Aachen, Germany¹⁶Fakultät Physik, Technische Universität Dortmund, Dortmund, Germany

- ¹⁷Max-Planck-Institut für Kernphysik (MPIK), Heidelberg, Germany
¹⁸Physikalisches Institut, Ruprecht-Karls-Universität Heidelberg, Heidelberg, Germany
¹⁹School of Physics, University College Dublin, Dublin, Ireland
²⁰INFN Sezione di Bari, Bari, Italy
²¹INFN Sezione di Bologna, Bologna, Italy
²²INFN Sezione di Ferrara, Ferrara, Italy
²³INFN Sezione di Firenze, Firenze, Italy
²⁴INFN Laboratori Nazionali di Frascati, Frascati, Italy
²⁵INFN Sezione di Genova, Genova, Italy
²⁶INFN Sezione di Milano, Milano, Italy
²⁷INFN Sezione di Milano-Bicocca, Milano, Italy
²⁸INFN Sezione di Cagliari, Monserrato, Italy
²⁹Università degli Studi di Padova, Università e INFN, Padova, Padova, Italy
³⁰INFN Sezione di Pisa, Pisa, Italy
³¹INFN Sezione di Roma La Sapienza, Roma, Italy
³²INFN Sezione di Roma Tor Vergata, Roma, Italy
³³Nikhef National Institute for Subatomic Physics, Amsterdam, Netherlands
³⁴Nikhef National Institute for Subatomic Physics and VU University Amsterdam, Amsterdam, Netherlands
³⁵AGH—University of Science and Technology, Faculty of Physics and Applied Computer Science, Kraków, Poland
³⁶Henryk Niewodniczanski Institute of Nuclear Physics Polish Academy of Sciences, Kraków, Poland
³⁷National Center for Nuclear Research (NCBJ), Warsaw, Poland
³⁸Horia Hulubei National Institute of Physics and Nuclear Engineering, Bucharest-Magurele, Romania
³⁹Affiliated with an institute covered by a cooperation agreement with CERN
⁴⁰DS4DS, La Salle, Universitat Ramon Llull, Barcelona, Spain
⁴¹ICCUB, Universitat de Barcelona, Barcelona, Spain
⁴²Instituto Galego de Física de Altas Enerxías (IGFAE), Universidade de Santiago de Compostela, Santiago de Compostela, Spain
⁴³Instituto de Física Corpuscular, Centro Mixto Universidad de Valencia—CSIC, Valencia, Spain
⁴⁴European Organization for Nuclear Research (CERN), Geneva, Switzerland
⁴⁵Institute of Physics, Ecole Polytechnique Fédérale de Lausanne (EPFL), Lausanne, Switzerland
⁴⁶Physik-Institut, Universität Zürich, Zürich, Switzerland
⁴⁷NSC Kharkiv Institute of Physics and Technology (NSC KIPT), Kharkiv, Ukraine
⁴⁸Institute for Nuclear Research of the National Academy of Sciences (KINR), Kyiv, Ukraine
⁴⁹University of Birmingham, Birmingham, United Kingdom
⁵⁰H.H. Wills Physics Laboratory, University of Bristol, Bristol, United Kingdom
⁵¹Cavendish Laboratory, University of Cambridge, Cambridge, United Kingdom
⁵²Department of Physics, University of Warwick, Coventry, United Kingdom
⁵³STFC Rutherford Appleton Laboratory, Didcot, United Kingdom
⁵⁴School of Physics and Astronomy, University of Edinburgh, Edinburgh, United Kingdom
⁵⁵School of Physics and Astronomy, University of Glasgow, Glasgow, United Kingdom
⁵⁶Oliver Lodge Laboratory, University of Liverpool, Liverpool, United Kingdom
⁵⁷Imperial College London, London, United Kingdom
⁵⁸Department of Physics and Astronomy, University of Manchester, Manchester, United Kingdom
⁵⁹Department of Physics, University of Oxford, Oxford, United Kingdom
⁶⁰Massachusetts Institute of Technology, Cambridge, Massachusetts, USA
⁶¹University of Cincinnati, Cincinnati, Ohio, USA
⁶²University of Maryland, College Park, Maryland, USA
⁶³Los Alamos National Laboratory (LANL), Los Alamos, New Mexico, USA
⁶⁴Syracuse University, Syracuse, New York, USA
⁶⁵School of Physics and Astronomy, Monash University, Melbourne, Australia
^(associated with Department of Physics, University of Warwick, Coventry, United Kingdom)
⁶⁶Pontifícia Universidade Católica do Rio de Janeiro (PUC-Rio), Rio de Janeiro, Brazil
^{(associated with Universidade Federal do Rio de Janeiro (UFRJ), Rio de Janeiro, Brazil)}
⁶⁷Physics and Micro Electronic College, Hunan University, Changsha City, China
^(associated with Institute of Particle Physics, Central China Normal University, Wuhan, Hubei, China)
⁶⁸Guangdong Provincial Key Laboratory of Nuclear Science, Guangdong-Hong Kong Joint Laboratory of Quantum Matter, Institute of Quantum Matter, South China Normal University, Guangzhou, China
^(associated with Center for High Energy Physics, Tsinghua University, Beijing, China)
⁶⁹Lanzhou University, Lanzhou, China
^{(associated with Institute Of High Energy Physics (IHEP), Beijing, China)}

- ⁷⁰School of Physics and Technology, Wuhan University, Wuhan, China
 (associated with Center for High Energy Physics, Tsinghua University, Beijing, China)
- ⁷¹Departamento de Fisica, Universidad Nacional de Colombia, Bogota, Colombia
 (associated with LPNHE, Sorbonne Université, Paris Diderot Sorbonne Paris Cité, CNRS/IN2P3, Paris, France)
- ⁷²Universität Bonn—Helmholtz-Institut für Strahlen und Kernphysik, Bonn, Germany
 (associated with Physikalisches Institut, Ruprecht-Karls-Universität Heidelberg, Heidelberg, Germany)
- ⁷³Eotvos Lorand University, Budapest, Hungary
 (associated with European Organization for Nuclear Research (CERN), Geneva, Switzerland)
- ⁷⁴INFN Sezione di Perugia, Perugia, Italy
 (associated with INFN Sezione di Ferrara, Ferrara, Italy)
- ⁷⁵Van Swinderen Institute, University of Groningen, Groningen, Netherlands
 (associated with Nikhef National Institute for Subatomic Physics, Amsterdam, Netherlands)
- ⁷⁶Universiteit Maastricht, Maastricht, Netherlands
 (associated with Nikhef National Institute for Subatomic Physics, Amsterdam, Netherlands)
- ⁷⁷Tadeusz Kosciuszko Cracow University of Technology, Cracow, Poland
 (associated with Henryk Niewodniczanski Institute of Nuclear Physics Polish Academy of Sciences, Kraków, Poland)
- ⁷⁸Department of Physics and Astronomy, Uppsala University, Uppsala, Sweden
 (associated with School of Physics and Astronomy, University of Glasgow, Glasgow, United Kingdom)
- ⁷⁹University of Michigan, Ann Arbor, Michigan, USA
 (associated with Syracuse University, Syracuse, New York, USA)
- ⁸⁰Departement de Physique Nucléaire (SPhN), Gif-Sur-Yvette, France

^aDeceased.^bAlso at Università di Roma Tor Vergata, Roma, Italy.^cAlso at Università di Firenze, Firenze, Italy.^dAlso at Scuola Normale Superiore, Pisa, Italy.^eAlso at Università di Ferrara, Ferrara, Italy.^fAlso at Università di Milano Bicocca, Milano, Italy.^gAlso at Università di Bologna, Bologna, Italy.^hAlso at Università di Genova, Genova, Italy.ⁱAlso at Universidade da Coruña, Coruña, Spain.^jAlso at Universidad Nacional Autónoma de Honduras, Tegucigalpa, Honduras.^kAlso at Centro Federal de Educacão Tecnológica Celso Suckow da Fonseca, Rio De Janeiro, Brazil.^lAlso at Università di Bari, Bari, Italy.^mAlso at Università di Cagliari, Cagliari, Italy.ⁿAlso at Università di Perugia, Perugia, Italy.^oAlso at Università degli Studi di Milano, Milano, Italy.^pAlso at LIP6, Sorbonne Université, Paris, France.^qAlso at Universidade Federal do Triângulo Mineiro (UFTM), Uberaba-MG, Brazil.^rAlso at Universidade de Brasília, Brasília, Brazil.^sAlso at Hangzhou Institute for Advanced Study, UCAS, Hangzhou, China.^tAlso at Università di Pisa, Pisa, Italy.^uAlso at Central South University, Changsha, China.^vAlso at Università di Padova, Padova, Italy.^wAlso at Excellence Cluster ORIGINS, Munich, Germany.^xAlso at Università della Basilicata, Potenza, Italy.^yAlso at Universidad de Alcalá, Alcalá de Henares, Spain.^zAlso at Università di Urbino, Urbino, Italy.